Contents lists available at SciVerse ScienceDirect

CIRP Annals Manufacturing Technology

Journal homepage: www.elsevier.com/locate/cirp

Upflow Mitigation Strategy for Nested Printing

Yunxia Chen[a], Steven Chase Allo[a], Bing Ren[a], Yuetong Wu[b], Hitomi Yamaguchi (1)[a], Yong Huang[a,*]

[a] Department of Mechanical and Aerospace Engineering, University of Florida, Gainesville, FL 32611, United States of America
[b] Department of Industrial and Systems Engineering, University of Florida, Gainesville, FL 32611, United States of America

Embedded printing enables the fabrication of integrated and enveloped internal geometries. Upflow, a geometrical deviation resulting from nozzle-translation-induced hydrodynamics, may affect the printing accuracy during embedded printing, in particular, nested printing where multiple layers are disturbed simultaneously during embedded printing internally nested structures within pre-deposited yield-stress structures. For the first time, this study identifies and characterizes two distinct upflow patterns including the interfacial upflow between the depositing and enclosure matrices during nested printing. Furthermore, a four-step upflow mitigation strategy is proposed and evaluated, and its effectiveness is demonstrated in printing a brain limbic system with significantly improved printing fidelity.

Additive manufacturing, Optimization, Nested printing

1. Introduction

Embedded printing is an additive manufacturing process to print build material(s) into a support matrix, which is typically a yield-stress fluid. It can be employed to print complicated three-dimensional (3D) structures [1], channeled patterns, and functional devices/structures [2] depending on how the support matrix and/or printed build material are removed or not after printing is complete [3-5]. While embedded printing is a promising fabrication approach for various soft material-based applications, the upflow phenomenon during embedded printing represents a common printing geometrical deviation [3,5,6]. Specifically, nozzle translation in the yield-stress matrix during printing causes flow disturbance and leads to the upward dragging of the depositing filament over a distance [7], which eventually introduces distortions and impacts the printing accuracy of final structures [3].

While the conventional embedded printing approach is capable of fabricating structures with independent embedded features, structures with intricately nested patterns such as biomimetic architectures resembling those found in organs like the brain [8] require advanced printing approaches. As such, nested printing, also known as nested embedded printing, has been practiced in printing such structures. For nested printing, both the support matrix (named as the global matrix herein) and build material inks typically are yield-stress fluids (except the last ink). Specifically, the nested printing process involves the printing of a yield-stress ink in a yield-stress matrix, and the embeddedly printed yield-stress structure is further utilized as a yield-stress matrix for the sequential printing of a nested pattern in it; this process may continue per the design of nested structures. As expected, the upflow phenomenon may cause more challenges during the embedded printing of nested structures since multiple nested matrices may be affected due to the nozzle movement. Thus far, only the upflow phenomenon during the typical embedded printing process has been reported and characterized with some simulation and experimental efforts [9-11]; there are no systematic efforts and strategies devoted to mitigating the impact of upflow on printing fidelity. Furthermore, the upflow phenomenon may become more complicated during nested printing and result in observable defects [5], which is still to be characterized.

This study aims to characterize and mitigate the nested printing-induced upflow phenomenon by systematically identifying, characterizing, and further mitigating upflow patterns during nested printing. First, the characterization of two distinct patterns of upflow is performed, and the analysis of the effects of printing conditions and material properties on the upflow phenomenon is conducted. Then a strategy is proposed to mitigate the effects of the upflow phenomenon. Finally, the proposed mitigation strategy is validated in the nested printing of a brain limbic system featuring intricately nested architectures, including the cortex, cingulate gyrus, thalamus, and corpus callosum.

2. Nested printing

2.1. Nested printing mechanism

During nested printing, a special implementation format of embedded printing, the localized yield-stress matrix material around the nozzle undergoes a transition from solid to liquid due to the yield-stress fluid property of the matrix upon the nozzle movement-induced shear stress, facilitating ink deposition [3]. After the nozzle traverses over this region, the disappearance of the stress prompts the matrix to revert to the solid state, effectively entrapping the deposited feature as illustrated in the inset of Fig. 1a, which is also commonly encountered during embedded printing. As shown in Fig. 1a, during nested printing, a depositing structure is printed into a depositing matrix, which is a pre-existing structure embedded in an enclosure matrix. It should be noted that, the global matrix is also known as the overall enclosure matrix at the beginning of a nested printing process. As such, a previously deposited ink-based structure functions as a yield-stress matrix (depositing matrix) for subsequently embedded structure(s) (depositing structure(s)). This uniquely enables the three-dimensional (3D) fabrication of complex enveloped internal structures.

2.2. Upflow phenomenon and patterns

For typical embedded printing applications, the upflow is exclusively studied during the deposition of filaments. However, the upflow scenario during nested printing is more intricate due to the yield-stress fluid property inherent in both the global matrix and inks, causing both the dispensed feature and interfacial surface between the depositing and enclosure matrices to experience displacement and/or distortion, which further affect the printing fidelity.

As shown in Fig. 1b, the upflow phenomenon during nested printing can be mainly summarized in two patterns: depositing upflow (Fig. 1b(i)) and interfacial upflow (Fig. 1b(ii)). The depositing upflow can be characterized in terms of the filament displacement and filament distortion. During deposition, part of the depositing matrix around the dispensing nozzle is liquified due to the stress introduced by the nozzle movement, which may produce a differential hydrodynamic pressure around the feature being dispensed, lifting the deposited feature upward (the A-A view of Fig. 1b(i)). Consequently, the deposited feature deviates to be above the intended location or nozzle exit plane, which is classified as filament displacement (Video). At the same time, the deposited feature may undergo deformation, forming a waterdrop cross-section shape, which is classified as filament distortion.

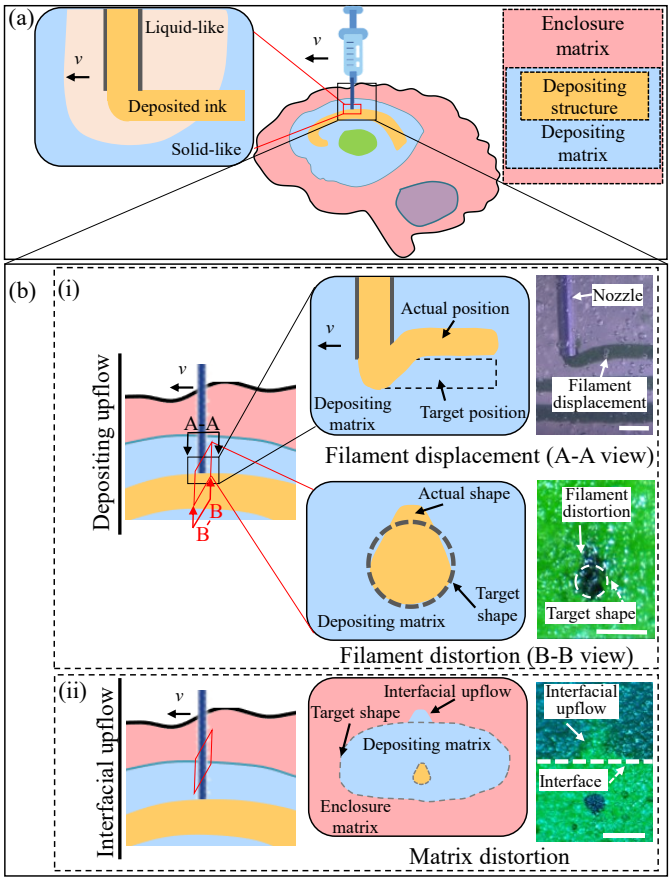

Fig. 1. Overall concept of nested printing technique and the associated upflow phenomenon. (a) Mechanism of nested printing. (b) Schematics of (i) depositing upflow and its related filament displacement and distortion and (ii) interfacial upflow and its related depositing matrix distortion. The A-A view image appears to have a different color because it is taken three-dimensionally during printing in a translucent matrix while the other two are based on the cross sections after printing. (Scale bars: 1 mm)

The interfacial upflow pattern occurs as a spike at the interface between the depositing and enclosure matrices where the yield-stress depositing matrix undergoes deformation due to repetitive nozzle disturbance. Consequently, the depositing matrix may become distorted, penetrating in the enclosure matrix above (Fig. 1b(ii)) similarly due to the nozzle movement-induced differential hydrodynamic pressure.

Given the heightened complexity of the upflow issue during nested printing, which involves multiple layers of matrices and the generation of intricate internal structures, the development of upflow mitigation strategy is imperative to ensure printing fidelity.

3. Upflow characterization and mitigation strategy

3.1 Characterization of upflow during nested printing

To assess the multifactorial effects of printing conditions (such as the printing speed, nozzle diameter, and flow rate) and material properties (including the ink/matrix relative viscosity and relative particle size of the microgel-based yield-stress matrix and ink materials) on the depositing and interfacial upflows, various quantitative parameters are proposed during the extrusion nested printing of filaments. Specifically, longitudinal images are captured to determine the filament displacement due to the depositing upflow, cross-sectional images of printed filaments are taken to evaluate the filament distortion due to the depositing upflow, and the interfacial area between the depositing and enclosure matrices are acquired to examine the distortion of two adjacent matrices due to the interfacial upflow.

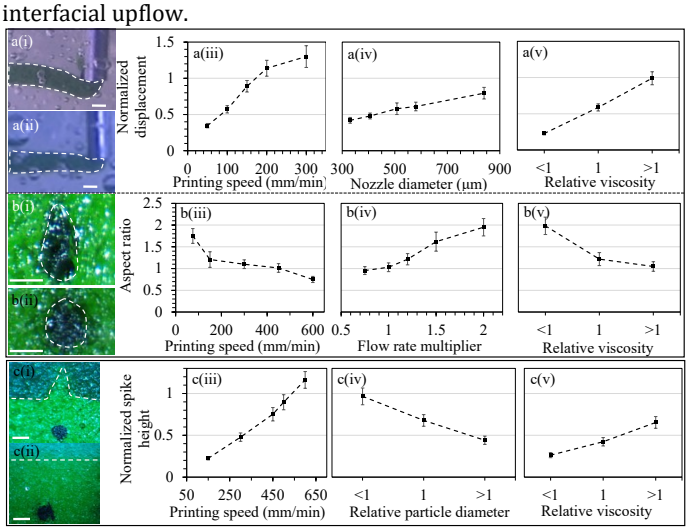

Fig. 2. Printing-induced upflow under different conditions. (a-c) Filament displacement due to the depositing upflow, filament distortion due to the depositing upflow, and matrix distortion due to the interfacial upflow, respectively. For each group, (i) a filament or matrices with the upflow-induced displacement or distortion, (ii) a filament or matrices with the upflow effect mitigated, (iii-v) the effects of printing conditions and material properties. (Scale bars: 500 μm and error bars: +/- one sigma)

Herein, a normalized filament displacement ($U_{Displacement}$) due to the depositing upflow is proposed by dividing the upward displacement of the filament ($h_{Filament}$) with respect to the horizontal plane of the dispensing nozzle outlet (h_{Nozzle}) by the nozzle diameter (d_{Nozzle}) as follows:

$$U_{Displacement} = (h_{Filament} - h_{Nozzle})/d_{Nozzle} \quad (1)$$

When there is no differential pressure-induced upflow, the top surface of filaments is expected to be approximately at the same height as the nozzle outlet plane with some die swelling-induced deviation. The upward displacement is defined as the distance from the top surface of the filaments to the nozzle outlet plane. For comparison, Fig. 2a(i-ii) shows the filament displacement

under the upflow effect and the upflow effect mitigated, respectively. Experimental observations reveal that the increase of the printing speed, nozzle diameter, and/or ink/matrix relative viscosity increases the normalized filament displacement, adversely impacting the printing fidelity as depicted in Fig. 2a(iii-v).

Furthermore, the filament distortion due to the depositing upflow is quantified using an aspect ratio $U_{Distortion}$, which is defined as the filament height ($h_{Filament}$) divided by its width ($w_{Filament}$) in the cross-sectional image of printed filaments (Fig. 2b(i-ii)) as follows:

$$U_{Distortion}=h_{Filament}/w_{Filament} \quad (2)$$

with an aspect ratio of 1 indicative of the most accurate structure, which is expected for robust printing applications. As depicted in Fig. 2b(iii-v), both the printing speed and ink/matrix relative viscosity adversely impact the aspect ratio, whereas the flow rate exhibits a positive influence on the aspect ratio.

The assessment of the effects of the interfacial upflow (Fig. 2c(i-ii)) utilizes a normalized spike height at the interfacial region ($U_{Interfacial}$) as the height of the spike (h_{Spike}) divided by the nozzle diameter (d_{Nozzle}) as follows:

$$U_{Interfacial} = h_{Spike}/d_{Nozzle} \quad (3)$$

which is influenced by factors such as the printing speed, ink/matrix relative particle size, and relative viscosity. A small normalized spike height is expected for high-fidelity printing. As depicted in Fig. 2c(iii-v), both the increase of the printing speed and ink/matrix relative viscosity leads to a larger normalized spike height of the distorted region, while the increase of the ink/matrix relative particle size results in a reduced normalized spike height.

3.2 Upflow mitigation strategy

To mitigate the effects of the aforementioned upflows on the printing fidelity during nested printing, a strategic approach is proposed by systematically characterizing and minimizing the displacement and/or distortion due to various upflow patterns. With the knowledge of empirical results regarding the effects of printing conditions and materials properties on the aforementioned three outflow parameters ($U_{Displacement}$, $U_{Distortion}$, and $U_{Interfacial}$), Fig. 3a illustrates such a mitigation strategy for upflow effects during nested printing, and the details are further explained as follows.

First, the initial upflow mitigation is to minimize the filament displacement observed during ink deposition (depositing upflow) (Step 1). If the normalized filament displacement ($U_{Displacement}$) is much larger than a pre-specified threshold c (such as 0.10, representing a 10% filament displacement that can be ignored), printing conditions and/or material properties are to be tuned accordingly based on one or both of the following two options: decreasing the printing speed, nozzle diameter, and/or ink viscosity, and increasing the matrix viscosity until the c value condition is met. Second, the mitigation for filament distortion due to the depositing upflow is conducted similarly, based on the characterized filament distortion index $U_{Distortion}$ (Step 2). If the filament distortion index is much larger than 1, printing conditions and/or material properties are to be tuned by either decreasing the flow rate multiplier and/or matrix viscosity and/or increasing the printing speed and/or ink viscosity until $U_{Distortion}$ is close to 1 or as specified. Third, the mitigation strategy is oriented to minimize the interfacial upflow without ink deposition after the effects of the depositing upflow are sufficiently alleviated (Step 3). If the normalized spike height $U_{Interfacial}$ is much greater than 1 (such as 1.50 or as specified), one or both of the following two options should be adopted: the printing speed and/or relative viscosity are to be decreased, and the relative particle size ratio between the ink and matrix microgels is to be increased. Finally, geometrical design pre-compensation is considered to compensate for the volume increase in pre-existing structures due to deposited materials (Step 4).

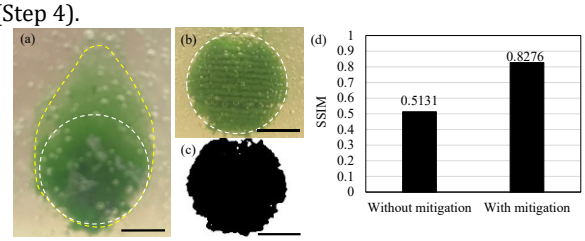

Fig. 3. Upflow mitigation results (solid sphere). (a) Without and (b) with upflow mitigation. (c) Processed printing results for SSIM analysis. (d) SSIM values for printed spheres without and with upflow mitigation. (Scale bars: 5 mm)

To evaluate the printing fidelity of printed objects after nested printing, geometrical errors were analyzed using a structural similarity (SSIM) index [12]. The index ranges from 0 to 1, and 1 means perfect shape fidelity. This analysis involves comparing cross-sectional images between the design and the printed objects before (Fig. 3b) and after applying the proposed upflow mitigation strategy (Fig. 3c). Images of the printed objects were converted into binary images (Fig. 3d) and then compared with the design using an SSIM program in MATLAB (MathWorks, MA, USA). The resulting SSIM values are shown in Fig. 3e, which shows the group with upflow mitigation has an SSIM value of 0.8276 while that without upflow mitigation is 0.5131, indicating the proposed upflow mitigation strategy efficiently improves the printing fidelity during nested printing.

4. Nested printing with upflow mitigation strategy

4.1 Yield-stress material design

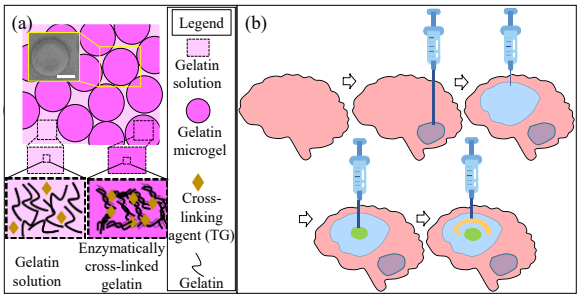

Fig. 4. Nested printing material and printing schematic. (a) Gelatin microgel-based composite with yield-stress fluid property as the ink and matrix material. (b) Design and printing process of the nested brain limbic system.

Successful nested printing generally requires the use of yield-stress materials for both inks and matrices. For the validation of the proposed upflow strategy for nested printing, a nested heterogeneous brain simulant is printed and further evaluated for print fidelity. Herein, a gelatin microgel-based composite is utilized as the foundational yield-stress build material, which comprises discrete gelatin microgels and a continuous gelatin solution with a cross-linking agent (transglutaminase (TG)) [13] as illustrated in Fig. 4a. The discrete solid phase of gelatin microgels contributes to refining the rheological and mechanical properties. The gelatin solution can undergo enzymatic cross-linking post-printing to ensure the integrity of each printed region within the overall system. The resulting gelatin composites exhibit solid-like properties until the yield stress surpasses the yield point. Upon yielding, the gelatin composite shows liquid-like

properties [13], indicating that it is a suitable material as both the matrix and ink for the validation study.

4.2 Design and printing process of brain simulant

The aforementioned yield-stress gelatin composite is utilized as the build material to print a brain simulant (the brain limbic system) using nested printing as illustrated in Fig. 4b. The gelatin composite was prepared using gelatin (Type A, MP Biomedicals, OH, USA) by following a protocol in a previous study [13]. For better visualization of distinct sections, natural dye powders (Natural Pigments, CA, USA) with a particle size of less than 4 μm were employed to color gelatin microgels.

Briefly, a 3D-scanned brain model (NIH3D, MD, USA) was first dissected to get regions like the cerebellum, cingulate gyrus, thalamus, and corpus callosum using Meshmixer (Autodesk, CA, USA) (Fig. 5a) and sliced using the integrated software on a Hyrel 3D printer (Hyrel3D, GA, USA). During this nested printing process, a gelatin composite was initially cast in a head surrogate with a brain-shape reservoir, serving as both the printing matrix and brain-cortex structure. Then a first gelatin composite ink was patterned within the cast yield-stress gelatin composite matrix, just like traditional embedded 3D printing. After the first structure in the matrix was deposited, the secondary complex-shaped structure was internally constructed using a second gelatin composite ink in the previously deposited structure, which is the pre-existing structure and serves as the depositing matrix for the secondary nested structure. Additional internal structures were deposited subsequently in a similar manner using distinct gelatin composites. After printing, the gelatin solution phase was enzymatically cross-linked by TG, resulting in the printed brain regions as an integrated system.

4.3 Printing fidelity evaluation

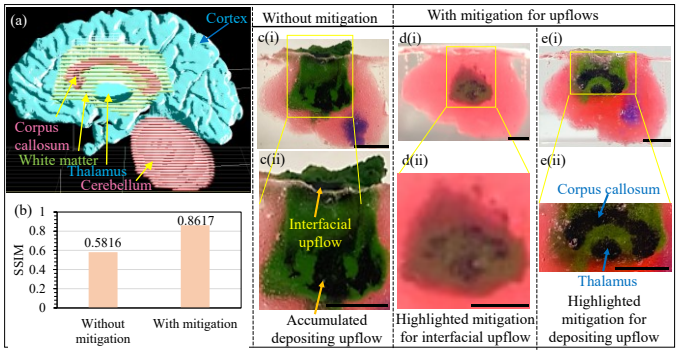

Fig. 5. Nested printing of brain simulant. (a) Brain simulant design. (b) SSIM values for printed brain simulants without and with upflow mitigation. (c) Brain simulant with visible geometrical deviations, (d) brain simulant printed with upflow mitigation (mitigated interfacial upflow is highlighted), and (e) brain simulant printed with upflow mitigation (mitigated depositing upflow is highlighted). (Scale bars: 1 cm)

For convenient qualitative assessment, cross-sectional images were taken and compared with those of the model of the brain and quantified using SSIM. This analysis involved comparing cross-sectional images between the designed model and the printed objects. The SSIM values of the nested brain limbic system before and after upflow mitigation are shown in Fig. 5b. The SSIM values are 0.5816 for the printing process without upflow mitigation but 0.8617 for that with upflow mitigation, demonstrating the effectiveness of the proposed upflow mitigation strategy in improving the printing fidelity. Fig. 5c-e further illustrates the printing fidelity enhancement upon the use of the mitigation strategy. In particular, the depositing and interfacial upflows are effectively minimized to achieve reasonable printing fidelity.

5. Conclusions and future work

This study has identified and characterized two distinct upflow patterns: depositing upflow and interfacial upflow due to the nozzle movement during nested printing. Depositing upflow introduces feature displacement and distortion, and interfacial upflow results in spike-like distortion between the depositing and enclosure matrices. To mitigate the effects of upflows on the printing fidelity, a heuristic four-step upflow mitigation strategy has been proposed and evaluated during nested printing, and the effectiveness of the strategy has been proved during the nested printing of a nested brain limbic system with significantly improved printing fidelity. While the proposed heuristic upflow mitigation strategy is effective, it has some main limitations. First, extensive experimental investigations are indispensable in order to get upflow characteristics, such as those in Fig. 2, that are needed to develop a strategy. Second, the values of the proposed normalized parameters (Eqs (1)-(3)) are not determined by considering the physical and rheological limits of material systems being printed. As such, they may not be optimal for the best mitigation performance. Future work may focus on understanding the underlying physics of the identified upflows during nested printing, quantitatively quantifying the printing fidelity by optimizing the slicing thickness and model reconstruction algorithm to establish an accurate reference printed geometry and refining the mitigation strategy quantitatively for better printing performance.

Acknowledgments

The research was partially supported by the University of Florida Claude D. Pepper Older Americans Independence Center P30AG028740, the U.S. National Institutes of Health (5R21HL162405), and the U.S. National Science Foundation (2233814).

References

[1] Chen, Y., Gao, Z., Hoo, S.A., Tipnis, V., Wang, R., Mitevski, I., Hitchcock, D., Simmons, K.L., Sun, Y.P., Sarntinoranont, M., Huang, Y., 2024, Sequential Dual Alignments Introduce Synergistic Effect on Hexagonal Boron Nitride Platelets for Superior Thermal Performance, Advanced Materials, p.2314097.

[2] Muth, J.T., Vogt, D.M., Truby, R.L., Mengüç, Y., Kolesky, D.B., Wood, R.J., Lewis, J.A., 2014, Embedded 3D Printing of Strain Sensors Within Highly Stretchable Elastomers, Advanced Materials, 26/36:6307-6312.

[3] Wu, Q., Song, K., Zhang, D., Ren, B., Sole-Gras, M., Huang, Y., Yin, J., 2022, Embedded Extrusion Printing in Yield-stress-fluid Baths, Matter, 5/11:3775-3806.

[4] Ren, B., Song, K., Chen, Y., Murfee, W.-L., Huang, Y., 2023, Laponite Nanoclay-modified Sacrificial Composite Ink for Perfusable Channel Creation via Embedded 3D Printing, Composites Part B: Engineering, 2023:110851.

[5] Alioglu, M.-A., Yilmaz, Y.-O., Singh, Y.-P., Nagamine, M., Celik, N., Kim, M.-H., Ozbolat, I.-T., 2023, Nested Biofabrication: Matryoshka-Inspired Intra-Embedded Bioprinting, Small Methods, 2023:2301325.

[6] Weeks, R.-D., Truby, R.-L., Uzel, S.-G., Lewis, J.-A., 2023, Embedded 3D Printing of Multimaterial Polymer Lattices via Graph-Based Print Path Planning, Advanced Materials, 35/5:2206958.

[7] LeBlanc, K.J., Niemi, S.R., Bennett, A.I., Harris, K.L., Schulze, K.D., Sawyer, W.G., Taylor, C., Angelini, T.E., 2016, Stability of High Speed 3D Printing in Liquid-like Solids, ACS Biomaterials Science & Engineering, 2/10:1796-1799.

[8] Tarricone, G., Carmagnola, I., Chiono, V., 2022, Tissue-Engineered Models of the Human Brain: State-of-the-Art Analysis and Challenges, Journal of Functional Biomaterials, 13/3:146.

[9] Friedrich, L.-M., Seppala, J.-E., 2021, Simulated Filament Shapes in Embedded 3D Printing, Soft Matter, 17/35:8027-8046.

[10] Friedrich, L.-M., Gunther, R.-T., & Seppala, J.-E, 2022, Suppression of Filament Defects in Embedded 3D Printing, ACS Applied Materials & Interfaces, 14/28:32561-32578.

[11] Prendergast, M.-E., Burdick, J.-A., 2022, Computational Modeling and Experimental Characterization of Extrusion Printing into Suspension Baths, Advanced Healthcare Materials, 11/7:2101679.

[12] Wang, Z., Bovik, A.-C., Sheikh, H.-R., Simoncelli, E.-P., 2004, Image Quality Assessment: from Error Visibility to Structural Similarity. IEEE Transactions on Image Processing, 13/4:600-612.

[13] Compaan, A.-M., Song, K., Chai, W., Huang, Y., 2020, Cross-linkable Microgel Composite Matrix Bath for Embedded Bioprinting of Perfusable Tissue Constructs and Sculpting of Solid Objects, ACS Applied Materials & Interfaces, 12/7:7855-7868.